PIBB 生物化学与生物物理进展
Progress in Biochemistry and Biophysics
2024, 51(4): 924~943
www.pibb.ac.cn

Knockdown of *BMI1* Enhances The Sensitivity of Cervical and Endometrial Cancer Cells to Paclitaxel*

ZHAO Yi-Ting[1,2,3)**], LIN Yan[3)**], YANG Wei-Li[2,3)**,***], CHEN Jun[1,3)***]

([1)]*Department of Chemoradiotherapy, the Affiliated People's Hospital of Ningbo University, Ningbo* 315000, China;
[2)]*Department of Gynecology, the Affiliated People's Hospital of Ningbo University, Ningbo* 315000, China;
[3)]*Department of Biochemistry and Molecular Biology, Zhejiang Key Laboratory of Pathophysiology, Health Science Center of Ningbo University, Ningbo* 315000, China)

Abbreviations: BLCA, Bladder urothelial carcinoma; BRCA, Breast invasive carcinoma; CCK-8, Cell Counting Kit-8; CESC, Cervical squamous cell carcinoma and endocervical adenocarcinoma; CHOL, Cholangiocarcinoma; COAD, Colon adenocarcinoma; COAD/READ, Colon adenocarcinoma/Rectum adenocarcinoma esophageal carcinoma; DLBC, Lymphoid neoplasm diffuse large B-cell lymphoma; DMEM, Dulbecco's Modified Eagle Medium; EC, Uterine corpus endometrial carcinoma; ESCA, Esophageal carcinoma; ECL, Enhanced Chemiluminescence; GBM, Glioblastoma multiforme; GBMLGG, Glioma; HNSC, Head and neck squamous cell carcinoma; KICH, Kidney chromophobe; KIPAN, Pan-kidney cohort (KICH+KIRC+KIRP); KIRC, Kidney renal clear cell carcinoma; KIRP, Kidney renal papillary cell carcinoma; LAML, Acute myeloid leukemia; LGG, Brain lower grade glioma; LIHC, Liver hepatocellular carcinoma; LUAD, Lung adenocarcinoma; LUSC, Lung squamous cell carcinoma; MESO, Mesothelioma; PAAD, Pancreatic adenocarcinoma; PCPG, Pheochromocytoma and paraganglioma; PRAD, Prostate adenocarcinoma; READ, Rectum adenocarcinoma; SARC, Sarcoma; STAD, Stomach adenocarcinoma; SKCM, Skin cutaneous melanoma; STES, Stomach and esophageal carcinoma; TGCT, Testicular germ cell tumors; THCA, Thyroid carcinoma; THYM, Thymoma; UCS, Uterine carcinosarcoma; UCEC, Uterine corpus endometrial carcinoma; UVM, Uveal melanoma; OS, Osteosarcoma; NB, Neuroblastoma; MESO, Mesothelioma; OV, Ovarian serous cystadenocarcinoma; T, Tumor; N, Normal; PTX, paclitaxel

Abstract **Objective** To study the effects of *BMI1* on the proliferation and drug resistance of cervical cancer (CC) and endometrial cancer (EC) cells. In addition, the mechanism of paclitaxel (PTX) resistance induced by BMI1 was explored. **Methods** In this study, we utilized the GTEx, Cbioportal, TCGA, and CPTAC databases to comprehensively analyze the mutation rate as well as mRNA and protein expression profiles of BMI1 in CC and EC. Subsequently, immunohistochemistry (IHC) analysis was employed to evaluate the protein expression levels of BMI1 in 40 pairs of CC and 40 pairs of EC tissue samples. Western blot was conducted to investigate alterations in downstream factor protein levels upon *BMI1* knockdown in CC and EC cells. Furthermore, functional experiments were performed to elucidate the role of BMI1 in CC and EC cells. Finally, we assessed the synergistic anti-growth effect by combining *BMI1* knockdown with paclitaxel treatment *in vitro*. **Results** The Cbioportal database revealed that *BMI1* amplification, misinterpretation, and splicing occurred in 1.5% of CC patients and 1.9% of EC patients. Mining the data from TCGA and CPTAC databases, high mRNA levels of *BMI1* were associated with the pathological type of CC and lower overall survival, and high protein levels of BMI1 were related to EC's pathological type and tumor grade. Furthermore, the BMI1 protein level is overexpressed in cancer tissues of CC and EC compared with normal tissues, as detected by IHC analysis. Besides, drug sensitivity experiments showed that overexpression of BMI1 resulted in decreased sensitivity of HeLa and HEC-1-A cells to a variety of anticancer drugs, including paclitaxel. In order to further analyze the relationship between BMI1 and paclitaxel resistance, Western blot was used to detect the changes in the protein levels of downstream factors of BMI1 in HeLa and HEC-1-A cells after *BMI1* knockdown. The results showed that the level of anti-apoptotic factor Bcl-2 protein decreased, while that of pro-apoptotic factor BAX increased with *BMI1* knockdown. Additionally, we showed that high expression of BMI1 promoted the proliferation and migration of CC and EC cells *in vitro*. Moreover, CC and EC cells with low BMI1 expression were more sensitive to the paclitaxel. **Conclusion** The expression of BMI1 is significantly upregulated in tumor tissues from patients with cervical and endometrial cancer, and silencing *BMI1* makes CC and EC cells more sensitive to paclitaxel *via* enhancing pro-apoptotic regulation.

* This work was supported by grants from The Medical and Health Science and Technology project of Zhejiang Province (2019RC274), Zhejiang Key Laboratory of Pathophysiology (202306), The Ningbo Natural Science Foundation (2021J017), Ningbo Public Welfare Science and Technology Plan Project (2021S116), and TCM Science and Technology Project of Zhejiang Province (2021ZB265).
** These authors contributed equally to this work.
*** Corresponding author.
YANG Wei-Li. Tel: 86-574-87017139, E-mail: gjywl-0506@163.com
CHEN Jun. Tel: 86-574-87017551, E-mail: cjcj992@163.com
Received: May 24, 2023 Accepted: October 16, 2023

Key words cervical cancer, endometrial cancer, BMI1, Bcl-2, paclitaxel
DOI：10.16476/j.pibb.2023.0207

Cervical cancer (CC) and endometrial cancer (EC) are two of the most common gynecologic malignant tumors in China and worldwide. CC in China accounts for 12% of the worldwide incidence of cervical cancer and 11% of cervical cancer-related deaths[1]. Globally, there were 382 000 new EC cases and 90 000 deaths in 2018, with an increasing incidence and decreasing age of onset[2-3]. Although the strategies for treating CC and EC are both based on clinical evaluation and stage, the primary treatment is surgery or chemoradiotherapy for early or locally advanced stages[4-5]. Paclitaxel exerts its anticancer activity by influencing apoptosis pathways. Therefore, paclitaxel-based drugs are the primary chemotherapy regimen for advanced stages of CC and EC patients, however, this treatment strategy is effective in the beginning, but with drug resistance and adverse reactions observed[6].

BMI1, a critical member of the polycomb repressor complex 1 (PRC1), regulates gene silencing by restructuring chromatin conformation and is abnormally expressed in different types of cancer. Its expression is associated with cancer's occurrence, progression, and poor prognosis[7-12]. Although several studies have indicated that inhibition of BMI1 may be a therapeutic approach in both CC and EC[12-16], there is still a lack of evidence from clinic data of CC and EC patients and the relationship between BMI1 and paclitaxel-associated drug resistance.

Here, we demonstrated that BMI1 protein levels are significantly elevated in CC and EC patient tumors. In a CC and EC cell model, high BMI1 expression triggered the proliferation and migration of CC and EC cells, while low BMI1 expression inhibited these phenomena. In addition, paclitaxel and *BMI1* knockdown significantly suppressed cell proliferation. Importantly, *BMI1* knockdown had an additive effect on the paclitaxel-induced apoptosis of CC and EC cells. Western blot results showed that the expression of the anti-apoptotic protein Bcl-2 was up-regulated in HeLa and HEC-1-A cells treated with BMI1 siRNA and paclitaxel. Therefore, using paclitaxel-based drugs combined with targeting BMI1 may serve as a promising approach for CC and EC patients with high BMI1 levels.

1 Materials and methods

1.1 Patients and clinicopathological data

A uniformly standardized pan-cancer dataset from The Cancer Genome Atlas database (TCGA) database (PANCAN, *N*=10 535, *G*=60 499) was downloaded from the UCSC platform (https://xenabrowser.net/), and the expression data of ENSG00000168283 (*BMI1*) gene in 26 cancer species (GBM, GBMLGG, LGG, CESC, LUAD, COAD, ADREAD, BRCA, ESCA, STES, KIRP, KIPAN, STAD, PRAD, UCEC, HNSC, KIRC, LUSC, LIHC, THCA, READ, PAAD, PCPG, BLCA, KICH, and CHOL) were extracted and analyzed. The sample selection criteria were as follows: Normal solid tissue, primary blood derived cancer-peripheral blood, primary tumor. $Log_2(x+1)$ conversion for each expression tumor species with fewer than 3 samples in a single tumor species were eliminated, and the expression data of 26 tumor species were obtained. R software (version 3.6.4) was used to calculate the difference in expression between normal and tumor samples in these 26 tumors, and unpaired Student's *t*-test was used for difference significance analysis.

The mRNA expression of BMI1 in 304 CC and 546 EC cases was downloaded from the UCSC platform (https://xenabrowser.net/, project: TCGA-CESC/TCGA-UCEC, datatype: RNA-COUNTS). R software (version 3.6.4) was used to calculate the mRNA level differences in BMI1 between normal and tumor samples in CC and EC (R program: limma; ggplot2; ggpubr). R software (version 3.6.4) was used to calculate pairwise expression differences between paired normal and tumor samples in CC and EC tumors (R limma; ggpubr). Unpaired Wilcoxon Rank Sum and Signed Rank Tests were used to analyze the significance of differences.

Correlation analysis between *BMI1* mRNA levels and clinical features of CC and CE was performed using the UALCAN platform (http://ualcan.path.uab.edu/index.html, data type: TCGA database-UCEC/TCGA database-CESC, project: RNA-COUNTS). Correlation analysis between BMI1 protein expression and clinical features of CC and CE was performed using the UALCAN platform (http://ualcan.path.uab.edu/analysis-prot.html, data type: CPTAC-

UCEC, project: BMI1 (NP_005171.4: S251)).

1.2 Immunohistochemistry (IHC) analysis

Forty pairs of human CC tissue specimens and twelve pairs of EC tissue specimens were collected at the Affiliated People's Hospital of Ningbo University. Samples were obtained *via* surgical excision or biopsy. The selection criteria were as follows: (1) the samples were confirmed to be primary CC and EC by pathological diagnosis; (2) the patient had no history of other systemic malignancies. All patients provided signed informed consent, and the study was approved by the Ethics Committee of the Ningbo University School of Medicine.

Formalin-fixed tissue samples from the patients were cut into tissue blocks at room temperature. The tissue blocks were fixed with 4% paraformaldehyde for more than 24 h, and then dehydrated in ethanol of different concentrations, embedded in paraffin, and sectioned into 4 μm slices. Sections were dewaxed and hydrated in xylene and ethanol at different concentrations. Heat-mediated antigen recovery was performed on the sections using Tris-EDTA antigen retrieval solution (Biosharp, BL617A). An ultrasensitive S-P (Rabbit/Mouse) IHC Kit (Kit-9710, Fuzhou Mai Xin Biotechnology) was used for the next steps. Endogenous peroxidase activity was blocked with 3% H_2O_2 at room temperature. Next, the sections were sealed with 10% donkey serum for 15 min, mixed with BMI1 antibody (dilution 1∶50; Abcam, AB32160), and incubated overnight.

The sections were then treated with biotinylated goat-anti-rabbit/mouse IgG secondary antibodies (Fuzhou Maixin Biotech) for 30 min. The sections were then incubated with streptavidin and horseradish peroxidase (Fuzhou Maixin Biotechnology) for 1 h. Finally, 3,3'-diaminobenzidine (DAB-0031, Fuzhou Mailxin Biotechnology Co., Ltd.) was used for 1 min of staining. Each step was washed 3 times with 1× PBS for 3 times, 5 min each time. 1×PBS instead of the BMI1 antibody was used as a negative control. Two independent pathologists scored the sections by IHC staining. A semi-quantitative method was used to calculate the percentage of positive cells: ≤10%, 0 points; 11%−25%, 1 point; 26%−50%, 2 points; 51%−75%, 3 points; and >75%, 4 points. Dyeing degree score: colorless, 0 points; light yellow, 1 point; brown-yellow, 2 points; brown, 3 points. According to the sum of the two, 0 is divided into (−); 1−2 are divided into (+); 3−4 are divided into (++); 5−6 are divided into (+++); and 7 points (++++). Statistical analysis (−) was negative, (+) and (++) combined for weakly positive, and (+++) and (++++) combined with strong positive expression. Images were captured using an Olympus IX73 inverted fluorescence microscope and the accompanying software.

1.3 Cell lines and cell culture

The human embryonic kidney cell line (HEK-293T) and cervical CC line (HeLa) were obtained from American Type Culture Collection (ATCC). The human EC cell line (HEC-1-A) is a gift from Professor GAO Kun of Tongji University. HEK-293T and HeLa were cultured in Dulbecco's Modified Eagle Medium (DMEM, Meilunbio) with 10% fetal bovine serum (FBS Premium, PAN-Seratech). HEC-1-A cells were cultured in Dulbecco's Modified Eagle Medium:Nutrient Mixture F-12 (DMEM/F-12 (1∶1), Meilunbio) with 10% fetal bovine serum (FBS Premium, PAN-Seratech). All cells were grown at 37° C with 5% CO_2.

Similar to our previous study[17], the *BMI1* gene fragment was obtained from the cDNA sequence of HeLa cells using specific primers, and the BMI1 fragment and mammalian expression vector pCMV-Myc vector were excised using restriction endonucleases to obtain *Kpn*I/*Not*I sticky ends. This fragment was ligated into the vector to construct the pCMV-BMI1 plasmid. To achieve knockdown of the target gene, the shRNA sequence targeting BMI1 was sub-cloned into pLKO. 1-GFP-shRNA vectors. Primers and shRNA sequences are listed in Table S1. All constructs were verified by DNA sequencing.

All transfection experiments were performed using Lipo6000TM transfection reagent (cat#C0526; Beyotime, China), according to the manufacturer's instructions. Briefly, 105 cells were seeded in 6-well plates and transiently transfected with 3 μg of pCMV-myc-BMI1, siBMI1, or empty vector.

1.4 Western blot

Protein samples from each lysate of fresh cells treated with RIPA buffer (cat#R0010; Solarbio, China) were loaded and separated by 10% SDS-PAGE, and then transferred to Amersham Protran 0.2 μm nitrocellulose membranes. NC membranes were blocked with 5% fat-free milk for 1 h at room temperature. The membranes were probed with anti-BMI1 (cat#ab269678; Abcam, England), anti-BAX (cat#50599-2-Ig, Proteintech, America), anti-Bcl-2

(cat#12789-1-AP, Proteintech, America), anti-Cleaved PARP1 (cat#ab32064, Abcam, England), anti-Cleaved Caspase-3 (cat#ab32042, Abcam England), and anti-GAPDH (cat#A19056, Abclonal, China) at 4℃ overnight. The membranes were then incubated with HRP-conjugated anti-mouse or anti-rabbit immunoglobulin (cat#SA00001-1 and cat#SA00001-2, Proteintech, America) for 1 h at room temperature. Proteins of interest were visualized using an enhanced chemiluminescence (ECL) system (cat#412, Vazyme, China). Western blot was performed 2−3 times in at least two independent experiments, and representative pictures are shown.

1.5 Reverse transcription-quantitative PCR（RT-qPCR）

Total RNA was isolated from HeLa and HEC-1-A cells using TRIzol Reagent (cat#15596018, Thermo Fisher, USA), and cDNA was reverse-transcribed using HiScript III All-in-one RT SuperMix Perfect for qPCR (cat#R333, Vazyme, China) following the manufacturer's instructions. PCR amplification was performed using the Taq Pro Universal SYBR qPCR Master Mix (cat#Q712, Vazyme, China). All quantifications were normalized to the level of the endogenous control GAPDH. The primer sequences used for RT-qPCR are listed in Table S1. RT-qPCR was performed 2−3 times in at least two independent experiments, and representative pictures are shown.

1.6 Wound−healing closure assay

Cells were cultured in 6-well plate, and when the cells grew until they spread over the small wells, the linear wound was scratched with the tip of a 10 μl pipette. The medium was replaced with 2% FBS serum, a proliferation inhibitor (mitomycin C, GlpBio, USA) was added, and wound healing was observed under a microscope and photographed. After 48 h, wound healing was again observed under a microscope and photographed, and the degree of wound healing was statistically analyzed. Each analysis was performed in 3 replicates.

1.7 Transwell migration assay

Cells transfected with pCMV-Myc-BMI1, siBMI1, or the empty vector were cultured for 24 h. The cells were digested into a uniform single-cell suspension and centrifuged at 1 000 r/min for 4 min. The supernatant was discarded and the cells were resuspended in 1 ml of DMEM, counted on a cell counting plate, and diluted with DMEM as needed. Then, transwell chambers were placed into a 24-well cell plate, and 200 μl of the above single-cell suspension was added to the upper chamber to quantify 1×10^4 cells. Complete medium (500 μl) was added to the lower chamber and the plate was placed in a constant-temperature incubator after standing for 30 min. After 24 h, the medium was discarded and the cells were washed twice with PBS. Next, 500 μl of 4% paraformaldehyde fixing solution was added to the chamber and allowed to stand for 30 min. The fixing solution was discarded, the cells were washed twice with PBS, 500 μl of 0.1% crystal violet dye was added, and the plate was stained on a shaker for 20 min. After rinsing with PBS 3 times, the chamber was dried naturally, photos were taken, and statistics were obtained.

1.8 Cell proliferation assay

The Cell growth curves were determined using the Cell Counting Kit-8 (CCK-8) assay. Cell proliferation rates were determined using CCK-8 (cat#K1018, APExBIO, America) according to the manufacturer's protocol. Cells were seeded in 96-well plates at a density of 2 000 cells per well. On each of the seven consecutive days of seeding, 10 μl of CCK-8 solution was added to each cell culture and incubated for 2 h. The resulting color was measured at 450 nm wavelength using a microplate absorbance reader (Bio-Rad, Hercules, CA, USA). Each measurement was performed in triplicates.

1.9 Colony formation assay

A total of 2 000 cells in 2 ml of growth medium were plated in quadruplicate in a 6-well plate, and the growth medium was changed every 3−4 d. After 14 d, the cells were rinsed twice with PBS, fixed with 10% formaldehyde, and stained with crystal violet (cat# G1063, Solarbio, China). The number of colonies was counted. Each count was performed in triplicates.

1.10 Flow cytometry to detect apoptosis

Cells treated according to the experimental protocol were collected and enumerated, followed by obtaining a cell suspension containing 1×10^5 cells and adding 500 μl 1× binding buffer. The cells were then gently mixed and swirled before adding 5 μl each of Annexin V-FITC and PI staining solution to the cell suspension, which was incubated for 10 min. Flow cytometry was performed to assess apoptosis. The excitation wavelength for Annexin V-FITC detection was set at 494 nm with a maximum emission wavelength of 518 nm, while the PI detection parameters were set at 535 nm and transmitting

wavelength set at 617 nm, respectively. Analysis results revealed that double-negative normal cells were in the lower left quadrant of the scatter plot, whereas late apoptotic or necrotic cells can be found in the upper right quadrant as single positive cells in the lower right quadrant, where mechanically damaged cells are observed in the upper left quadrant. Apoptosis analysis and mapping were performed using the FlowJo version 10.0.

1.11 Statistical analysis

Statistical calculations were performed using GraphPad Prism software. Data are presented as *mean*±*SD* for experiments performed with at least 3 replicates. The differences between two groups were analyzed using Student's *t*-test, and multiple comparisons were performed using two-way analysis of variance (ANOVA). Statistical calculations of the transwell assay were performed using one-way ANOVA. Statistical calculations of IHC were performed using SPSS software. The Chi-squared test was used to analyze the differences between the two groups. * represents $P<0.05$; ** represents $P<0.01$; *** represents $P<0.001$; **** represents $P<0.000\ 1$.

2 Results

2.1 Expression of *BMI1* gene retrieved from bioinformatic databases

2.1.1 The mRNA level of BMI1 in human cancers from TCGA and GTEx database

To examine the role of BMI1 in pan-cancer, we downloaded a uniformly standardized TCGA pan-cancer dataset from the UCSC platform (https://xenabrowser.net/), from which we extracted the expression data of the ENSG00000168283 (*BMI1*) gene in each sample. We screened the following sample sources: normal solid tissue, primary blood-derived cancer-peripheral blood, and primary tumor. $Log_2(x+1)$ transformation was performed for each expression value. In addition, we also eliminated cancer species with less than three samples from a single cancer species and finally obtained the expression data of 26 cancer species. R software (version 3.6.4) was used to calculate the differences in expression between normal samples and tumor samples from these 26 tumors, and the unpaired Student's *t*-test was used for difference significance analysis. Significant upregulation was observed in COAD, COADREAD, BRCA, ESCA, STES, STAD, HNSC, LIHC, and CHOL, and significant downregulation was observed in KIRP, KIPAN, PRAD, UCEC, and KICH (Figure 1a, Table S2).

Furthermore, based on the analysis of the Genotype-Tissue Expression (GTEx) database, we observed a higher expression level of BMI1 in the cervical and ulters compared to other tissues (Figure 1b). These findings suggest that *BMI1* functions as an oncogene and may play a crucial role in cervical and endometrial cancer carcinogenesis. Subsequently, we obtained the CESC and UCEC datasets from the TCGA. The data sets were analyzed using R 4.2.1 platform, and Kaplan-Meier curves were generated. Our results demonstrated that patients with EC exhibiting high expression of BMI1 mRNA had significantly shorter overall survival (OS) compared to those with low expression levels (Figure 1c). However, no significant difference was observed in OS among patients with CC (Figure 1d).

Subsequently, we conducted a comprehensive analysis of BMI1 mRNA levels in CC and EC tissues. We compared BMI1 mRNA levels in 304 CC tumor specimens with 3 healthy cervical tissue specimens, and 546 EC tumor specimens with 35 healthy endometrial tissue specimens from the TCGA database. The comparison between CC tumor samples and healthy cervical tissues did not yield statistically significant differences due to the limited number of available healthy cervical tissue specimens (Figure S1a). In contrast, the mRNA level of BMI1 was significantly higher in normal endometrial tissues than in EC tissues (Figure S1b). Furthermore, we analyzed paired CC and EC samples from the TCGA database but found no significant difference in BMI1 transcriptional levels between normal and tumor tissues (Figure S1c, d).

2.1.2 The CC and EC cancer-associated BMI1 mutants from Cbioportal database

Given the limited increase in BMI1 mRNA levels observed in cancer within the TCGA database, we conducted a comprehensive analysis of genomic profile and copy number alterations to investigate the mutation landscape of *BMI1* in CC and EC. Utilizing Cbioportal mapping, we examined the OncoPrint representation of *BMI1* gene alterations in CC and EC samples from the TCGA dataset, revealing 1.9% or 1.5% instances of gene amplification missense mutations, and splice mutations among CC and EC patients (Figure 2a).

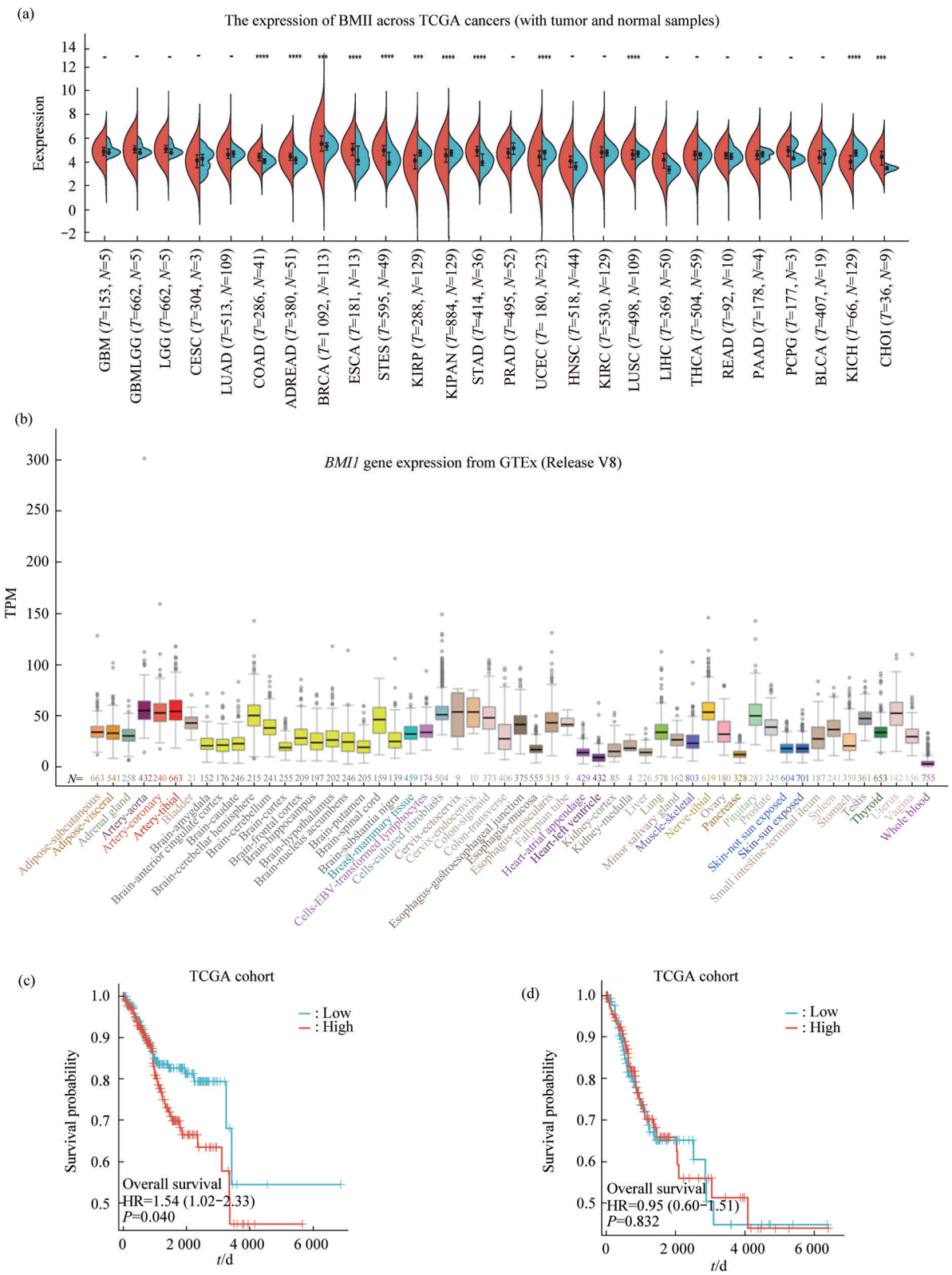

Fig. 1　The correlation between *BMI1* expression and overall survival analysis from TCGA and GTEx database

(a) The expression of *BMI1* in pan-cancer samples from TCGA database (tumor and normal samples). Significant upregulation was observed in COAD, COADREAD, BRCA, ESCA, STES, STAD, HNSC, LIHC, and CHOL, whereas significant downregulation was observed in KIRP, KIPAN, PRAD, UCEC, and KICH. ***P<0.001; ****P<0.000 1. (b) The expression of *BMI1* gene from GTEx database. (c) Kaplan-Meier curve of *BMI1* transcriptome and overall survival of EC patients in TCGA database (P=0.040). (d) Kaplan-Meier curve of *BMI1* transcriptome and overall survival of CC patients in TCGA database (P=0.832).

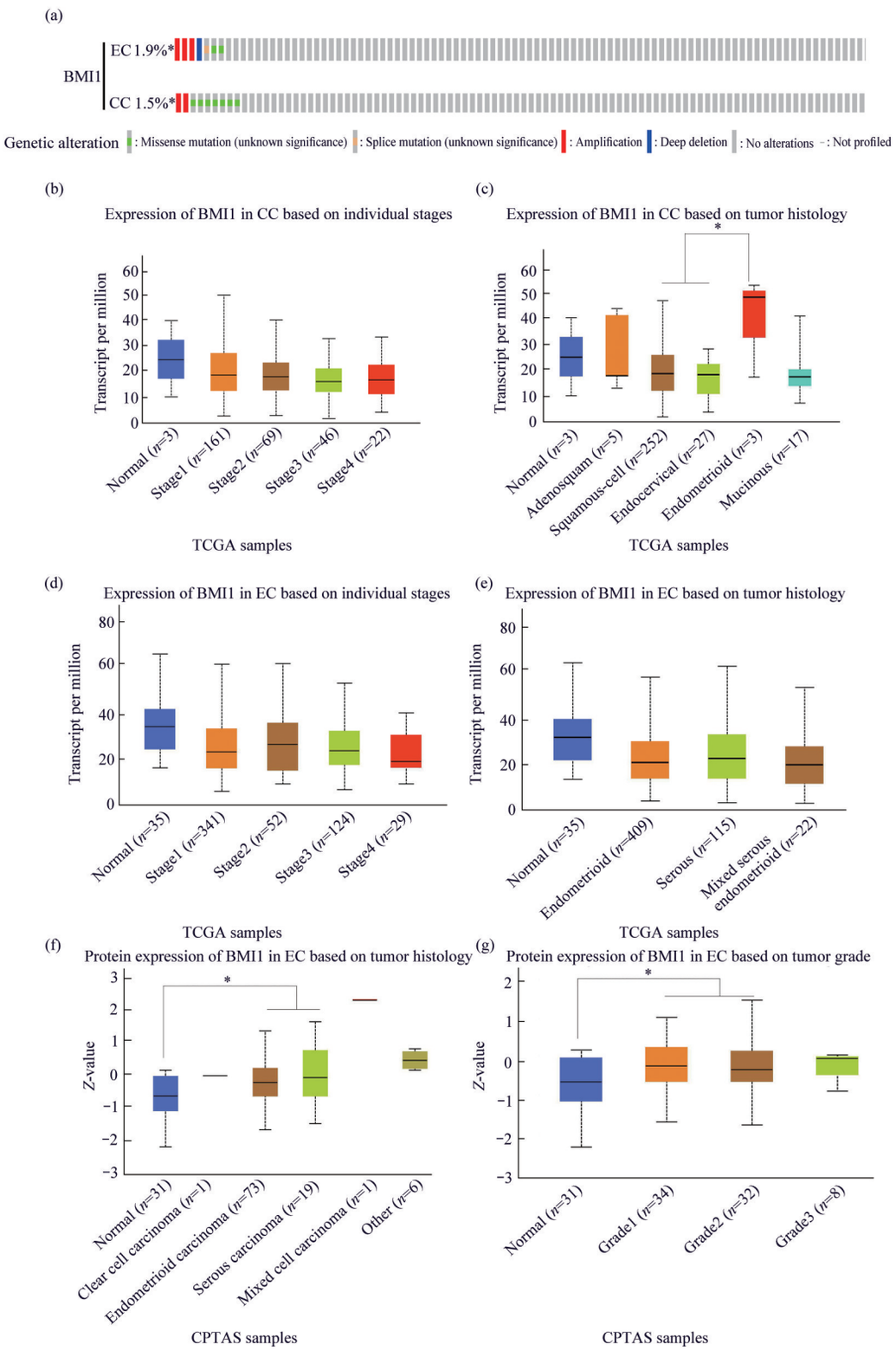

Fig. 2　The correlation between BMI1 expression and clinical features in CC and EC

(a) The Cbioportal OncoPrint map shows the distribution of BMI1 genomic changes in patients with endometrial and cervical cancer. (b) The expression of BMI1 in CC based on individual stages from TCGA database. The expression of BMI1 was not significantly correlated with the tumor stage of CC. (c) The expression of BMI1 in CC based on tumor histology from the TCGA database. The expression of BMI1 was significantly increased in the endometrioid adenocarcinoma subtype of CC compared to the squamous cell and endocervical subtypes. *P<0.05. (d) The expression of BMI1 in EC based on individual stages from TCGA database. (e) Expression of BMI1 in EC based on histology subtypes from TCGA database. (f) Protein expression of BMI1 in EC based on histology subtypes from the CPTAC database. BMI1 protein expression was higher in EC tissues than that in normal tissues. *P<0.05. (g) Protein expression of BMI1 in EC based on tumor grade from the CPTAC database. BMI1 protein is highly expressed in endometrioid carcinoma subtype and serous carcinoma subtype compared with normal tissues. *P<0.05.

2.1.3 The correlation between BMI1 and clinical features in CC and EC from the TCGA database

The UALCAN platform (http://ualcan.path.uab.edu/index.html) was used to analyze the correlation between BMI1 mRNA level and tumor stage and pathological type in CC and EC patients from the TCGA database (data type: TCGA-UCEC/TCGA-CESC, project: RNA-COUNTS). The transcription level of BMI1 was not significantly correlated with the tumor stage of CC but was related to the pathological type of CC. BMI1 mRNA levels were significantly increased in the endometrioid adenocarcinoma subtypes (Figure 2b, c). However, in EC, the transcription level of BMI1 was not significantly correlated with the tumor stage or the pathological type of EC (Figure 2d, e).

The UALCAN platform (http://ualcan.path.uab.edu/analysis-prot.html) was used to analyze the correlation between BMI1 protein expression and EC clinical features from the CPTAC database (data type: CPTAC-UCEC, project: BMI1 (NP_005171.4:S251)), and the results showed that BMI1 protein is highly expressed in endometrioid carcinoma and serous carcinoma subtypes compared with normal tissues (Figure 2f). In addition, higher BMI1 expression was associated with a high tumor grade in patients with EC (Figure 2g). However, data on the expression of the BMI1 protein in CC were not found in the CPTAC database.

2.2 The clinical significance of the BMI1 protein in CC and EC

2.2.1 Protein level of BMI1 in CC and EC tissues

Since the mRNA level of BMI1 in CC and EC samples from the TCGA database exhibits no significant difference, the protein level of BMI1 indicates potential clinical value. We next attempted to detect the expression level of BMI1 protein in CC and normal tissues using IHC analysis. BMI1 protein expression levels were significantly higher in CC tissues than in normal tissues (χ^2=25.1, P<0.001) (Figure 3a, b). A total of 52.5% (21/40) of CC tissues exhibited high expression of BMI1, whereas the other CC tissues (47.5%, 19/40) had negative or low expression levels of BMI1. In contrast, 2.5% (1/40) of normal CC tissues exhibited strong staining for BMI1, and 97.5% (39/40) exhibited negative and low staining.

Similarly, BMI1 protein expression levels were dramatically higher in EC tissues than in normal tissues (χ^2=35.32, P<0.000 1) (Figure 3a, c). A total of 65% (26/40) of EC tissues exhibited high BMI1 protein levels, whereas the other EC tissues (35%, 14/40) had negative or low expression levels of BMI1. In contrast, 2.5% (1/40) of normal EC tissues exhibited strong staining for BMI1, and 97.5% (39/40) exhibited negative or low staining. These findings indicated that the BMI1 protein level in CC and EC tissues was higher than that in normal CC and EC tissues.

2.2.2 Clinical value of BMI1 in CC and EC

The possible correlations between BMI1 protein expression and clinicopathological features in CC and EC tissues were evaluated. The protein level of BMI1 in CC tissues was closely related to the degree of pathological tumor differentiation (χ^2=34.9, P<0.001). There was no significant correlation between clinicopathological characteristics (age, height, weight, BMI, tumor size, tumor invasion depth, pathological type, TNM stage, FIGO stage, ER expression, and P16 expression) (Table 1). In EC tissues, the protein level of BMI1 was closely related to the degree of tumor pathological differentiation (χ^2=6.708, P=0.048) and the tumor invasion depth (χ^2=11.578, P=0.003). There was no significant correlation between clinicopathological characteristics (age, height, weight, BMI, tumor size, pathological type, TNM stage, FIGO stage, ER expression, and P16 expression) (Table 2).

2.3 BMI1 enhances the growth，proliferation，and migration of CC and EC cells

2.3.1 High expression of BMI1 *in vitro* promotes the growth and proliferation of CC and EC cells

To determine the potential functional role of BMI1 in CC and EC cell lines, we utilized the HeLa, and HEC-1-A cell lines. We transfected BMI1 and siBMI1 into these cells to increase the expression level of BMI1 or decreased ease the expression level of BMI1, respectively. The efficiency of siBMI1 was first determined by RT-qPCR in HeLa and HEC-1-A cells (Figure S2a, b). Further BMI1 protein expression was assessed using Western blot, and the results showed that BMI1 protein was successfully increased in HeLa and HEC-1-A cells overexpression BMI1, and decreased after transfection with siBMI1 (Figure 4a). The results of the CCK-8 assay showed that cell growth and proliferation were increased in BMI1-

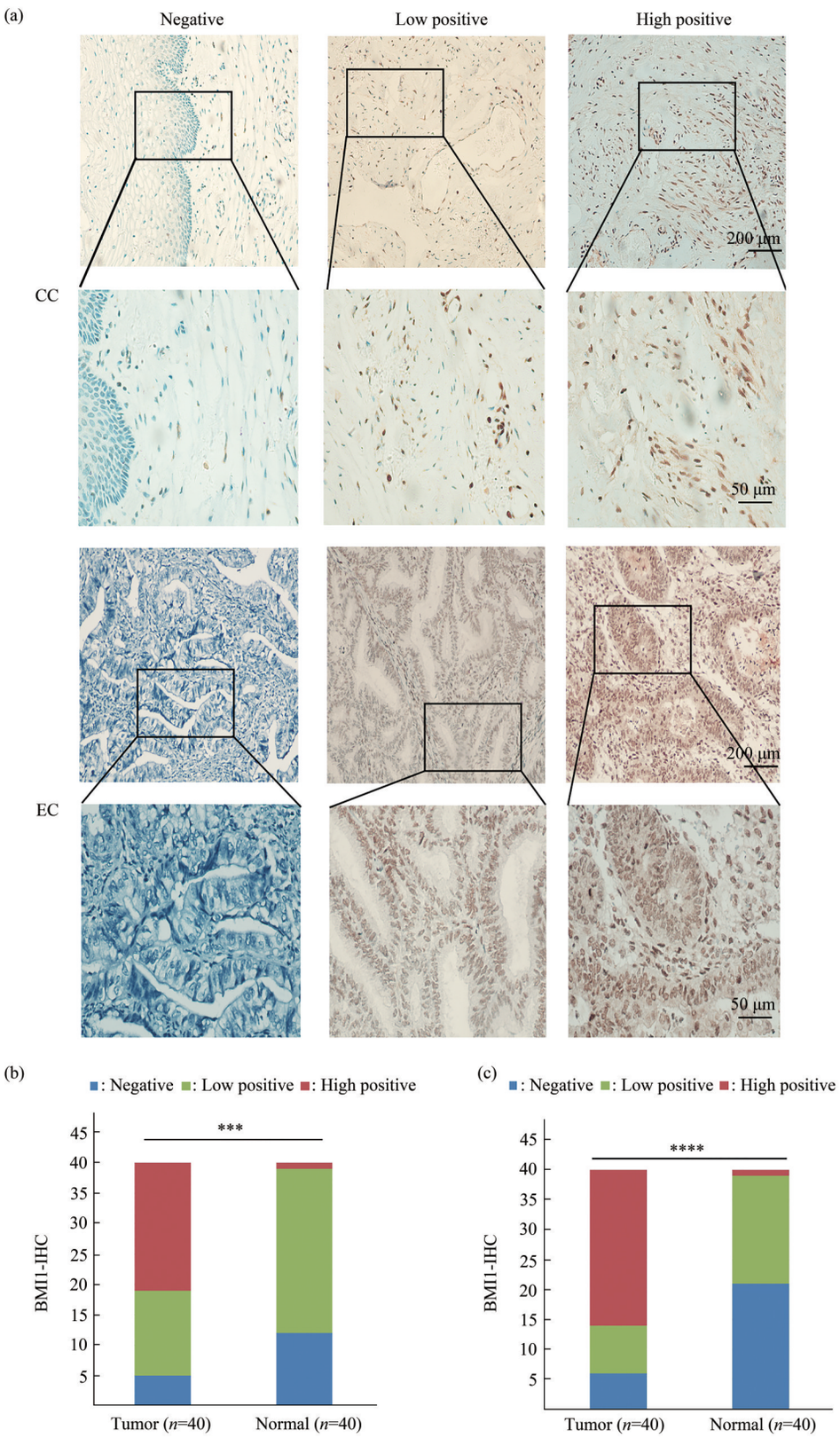

Fig. 3　BMI1 protein expression is elevated in CC and EC specimens

(a) Representative images of BMI1 IHC from 40 cases of CC and EC specimens. (b) Quantitative data of BMI1 protein staining in CC specimens. Statistical significance was determined by *Chi*-square test. ***P<0.001. (c) Quantitative data of BMI1 protein staining in EC specimens. Statistical significance was determined by *Chi*-square test. ****P<0.000 1.

Table 1　Expression level and clinical value of BMI1 in CC

Variables	Number	BMI1, *n* (%)			χ^2	*P*
		Negative	Low	High		
Age/years					0.911	0.634
<50	14	1 (7.14%)	7 (50%)	6 (42.8%)		
≥50	26	3 (11.5%)	8 (30.7%)	15 (57.6%)		
Height/cm					3.401	0.183
≤160	28	2 (7.1%)	13 (46.4%)	13 (46.4%)		
>160	12	2 (16.6%)	2 (16.6%)	8 (66.6%)		
Weight/kg					5.755	0.056
≤60	18	4 (22.2%)	5 (27.7%)	9 (50.0%)		
>60	22	0 (00.0%)	10 (45.4%)	12 (54.5%)		
BMI					5.455	0.065
<24	18	4 (22.2%)	6 (33.3%)	8 (44.4%)		
≥24	22	0 (00.0%)	10 (45.4%)	12 (54.5%)		
Race					—	—
Asian	40	5 (12.5%)	14 (35%)	21 (52.5%)		
White	0	0 (00.0%)	0 (00.0%)	0 (00.0%)		
Black and African	0	0 (00.0%)	0 (00.0%)	0 (00.0%)		
Tumor size/cm					0.833	0.659
<4	24	2 (10.0%)	8 (33.3%)	14 (58.3%)		
≥4	16	2 (12.5%)	7 (43.7%)	7 (43.7%)		
Infiltrating depth					2.449	0.294
<1/2 depth	14	2 (14.2%)	3 (21.4%)	9 (64.2%)		
≥1/2 depth	26	2 (7.69%)	12 (46.1%)	12 (46.1%)		
Histological type					1.401	0.496
Squamous cancer	34	3 (7.8%)	14 (41.1%)	17 (50.0%)		
Adenocarcinoma	6	1 (16.6%)	1 (16.6%)	4 (66.6%)		
Differentiation					**34.9**	**0.000 1**
Poor	6	0 (00.0%)	5 (83.3%)	1 (16.70%)		
Moderate	31	1 (3.2%)	10 (32.2%)	20 (64.5%)		
High	3	3 (100%)	0 (0.00%)	0 (0.00%)		
TNM stage					0.862	0.650
I	28	2 (7.1%)	11 (39.2%)	15 (53.5%)		
II	12	2 (16.6%)	4 (33.3%)	6 (50.0%)		
Local lymph node Metastasis					0.267 9	0.262
Negative	32	2 (6.4%)	12 (38.7.%)	18 (58.0%)		
Positive	8	2 (25%)	3 (37.5%)	3 (37.5%)		
FIGO stage					4.181	0.124
I	33	2 (5.4%)	14 (37.8%)	17 (56.7%)		
II	7	2 (28.5%)	1 (14.2%)	4 (57.1%)		
ER					1.556	0.459
Negative	8	1 (12.5%)	4 (50.0%)	3 (37.5%)		
Positive	6	0 (0.00%)	2 (33.3%)	4 (66.6%)		
P16					1.222	0.543
Negative	1	0 (0.00)	0 (0.00)	1 (100%)		
Positive	34	4 (11.7%)	15 (44.1%)	15 (44.1%)		

Table 2 Expression level and clinical value of BMI1 in EC

Variables	Number	BMI1, *n* (%)			χ^2	*P*
		Negative	Low	High		
Age/years					0.954	0.621
<50	7	2 (28.5%)	2 (28.5%)	3 (43%)		
≥50	33	5 (15.1%)	8 (24.2%)	20 (61.7%)		
Height/cm					2.151	0.341
≤160	24	3 (12.5%)	5 (20.8%)	16 (66.7%)		
>160	16	4 (25.0%)	5 (31.2%)	7 (43.8%)		
Weight/kg					2.888	0.236
≤60	15	2 (13.3%)	6 (40.00%)	7 (46.7%)		
>60	25	5 (20.0%)	4 (16.0%)	16 (64.0%)		
BMI					0.238	0.888
<24	26	5 (19.2%)	6 (23.0%)	15 (57.7%)		
≥24	14	2 (14.3%)	4 (28.5%)	8 (57.1%)		
Race					—	—
Asian	40	7 (17.5%)	10 (25%)	23 (57.5%)		
White	0	0 (0.00)	0 (0.00)	0 (0.00)		
Black and African	0	0 (0.00)	0 (0.00)	0 (0.00)		
Tumor size/cm					0.747	0.688
<4	21	3 (14.3%)	6 (28.5%)	12 (57.1%)		
≥4	19	4 (10.0%)	4 (10.0%)	11 (57.8%)		
Infiltrating depth					**6.078**	**0.048**
<1/2 depth	13	5 (21.1%)	3 (23.0%)	5 (38.5%)		
≥1/2 depth	27	2 (7.4%)	7 (25.9%)	18 (67.7%)		
Differentiation					**11.578**	**0.003**
Poor	15	6 (40.0%)	5 (33.3%)	4 (26.7%)		
Moderate-High	25	1 (4.0%)	5 (20.0%)	19 (76.0%)		
TNM stage					3.913	0.141
I	28	7 (25.0%)	7 (25.0%)	14 (50.0%)		
II	12	0 (0.00)	3 (25.0%)	9 (75.0%)		
FIGO stage					3.913	0.141
I	28	7 (25.0%)	7 (25.0%)	14 (50.0%)		
II	12	0 (0.00)	3 (25.0%)	9 (75.0%)		
ER					—	—
Negative	0	0 (0.00)	0 (0.00)	0 (0.00)		
Positive	9	0 (0.00)	0 (0.00)	9 (100%)		
P16					—	—
Negative	0	0 (0.00)	0 (0.00)	0 (0.00)		
Positive	10	0 (0.00)	1 (10%)	9 (90%)		

transfected cells but decreased in siBMI1-transfected HeLa and HEC-1-A cells compared to the respective controls (Figure 4b). In addition, the results of the HeLa and HEC-1-A cell colony formation assays showed that high expression of BMI1 promoted cell growth and proliferation, wherea low expression of BMI1 inhibited cell growth and proliferation (Figure 4c).

2.3.2 High expression of BMI1 *in vitro* promotes migration of CC and EC cells

The effect of BMI1 on cell migration was assessed using transwell migration assay (Figure 4d). The results showed that high expression of BMI1 promoted cell migration, while low expression of BMI1 inhibited cell migration. In addition, the same results were obtained from the wound-healing closure assay. The results showed that high expression of BMI1 promoted the migration of HeLa and HEC-1-A

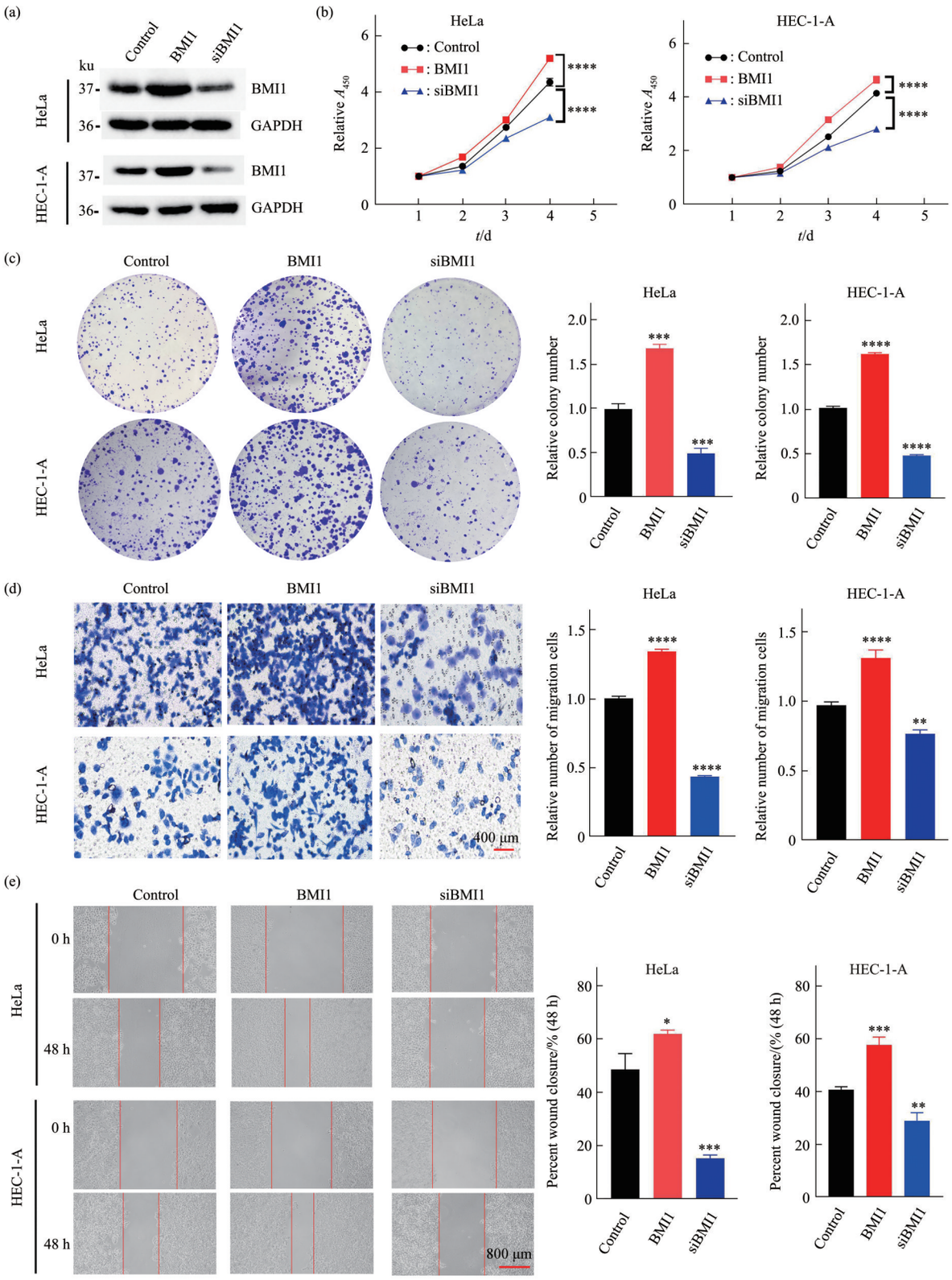

Fig. 4　Effect of BMI1 on the growth proliferation and migration invasion of HeLa and HEC−1−A cells

(a) Western blot of HeLa and HEC-1-A cells transfected with empty plasmids, BMI1 and siBMI1 plasmids. (b) Cell proliferation assay of HeLa and HEC-1-A cells transfected with empty plasmids, BMI1 and siBMI1 plasmids. Statistical analysis was performed using two-way ANOVA. ****P< 0.000 1. (c) Cell colony formation assay of HeLa and HEC-1-A cells transfected with empty plasmids, BMI1 and siBMI1 plasmids, all data shown are *mean*±*SD* (n=3). ***P<0.001; ****P<0.000 1. (d) Transwell migration assay of HeLa and HEC-1-A cells transfected with empty plasmids, BMI1 and siBMI1 plasmids. Statistical analysis of transwell assay was performed using one-way ANOVA. **P<0.01 ****P<0.000 1. (e) Wound healing at 48 h in the wound-healing closure assay. Statistical analysis of wound healing area data is shown as *mean*±*SD* (n=3). *P<0.05 **P<0.01; ***P<0.001.

cells after 48 h of culture, whereas downregulation of BMI1 significantly reduced the migration of HeLa and HEC-1-A cells (Figure 4e). These results together prove the role of BMI1 in promoting the migration of CC and EC cells.

2.4 BMI1 expression promotes drug resistance of CC and EC cells

We further investigated the potential role of BMI1 in promoting chemotherapeutic resistance. The results obtained from the chemotherapeutic drug sensitivity test assay demonstrated a significant increase in cell drug resistance among cells overexpressing BMI1 compared to their respective controls (Figure 5a, b). Overexpression of BMI1 confers differential resistance to doxorubicin, cisplatin, paclitaxel, raltitrexed, and oxaliplatin in

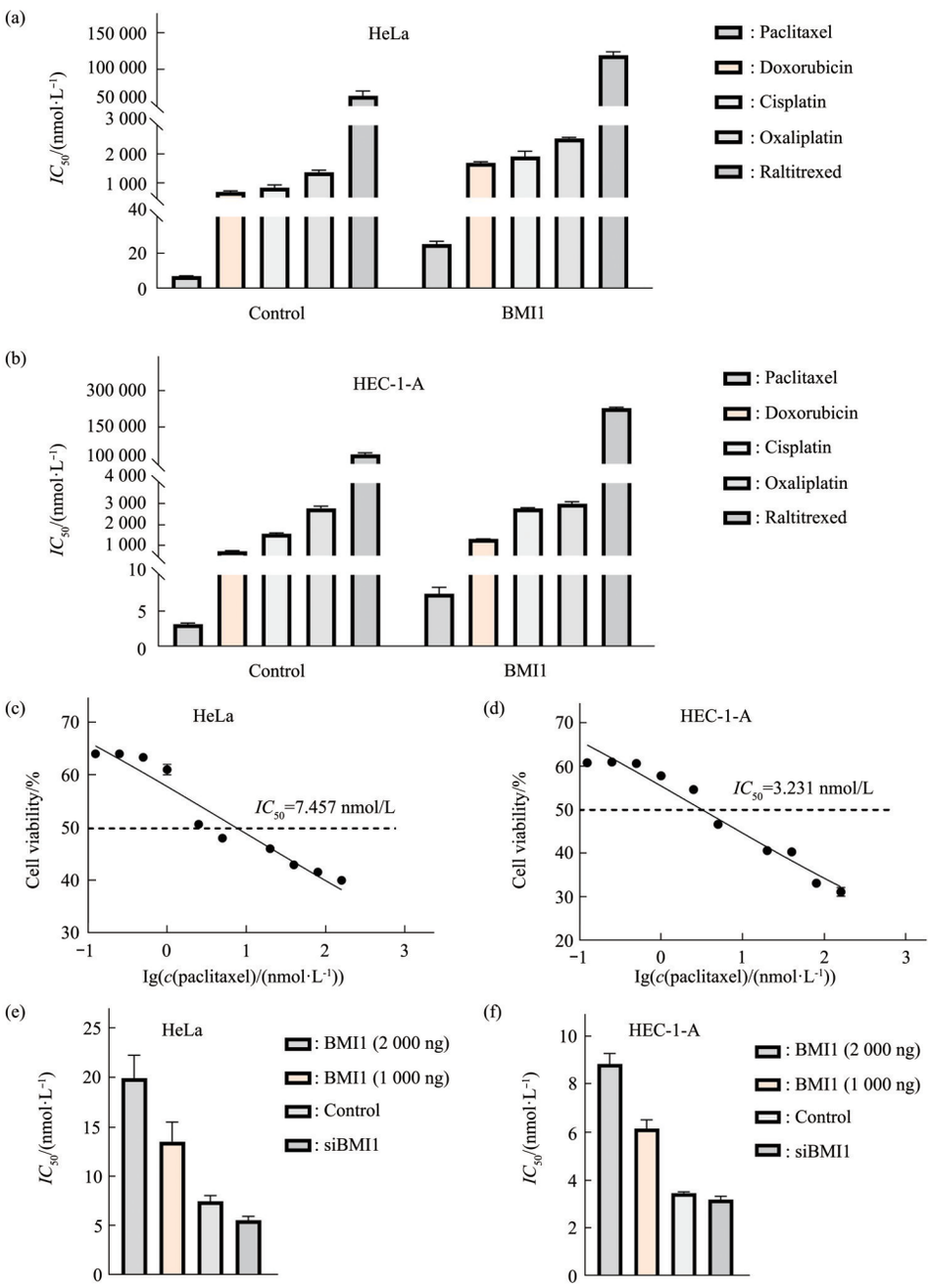

Fig. 5 BMI1 expression regulates anti−cancer drug tolerance of HeLa and HEC−1−A cells

(a) Sensitivity of HeLa cell line overexpressing BMI1 to antitumor drugs. (b) Sensitivity of HEC-1-A cell line overexpressing BMI1 to antitumor drugs. (c) IC_{50} value measured by applying paclitaxel to HeLa cells for 24 h. (d) IC_{50} value measured by applying paclitaxel to HEC-1-A cells for 24 h. (e) IC_{50} values by applying paclitaxel of HeLa cells under different expression levels of BMI1. (f) IC_{50} values by applying paclitaxel of HEC-1-A cells under different expression levels of BMI1.

HeLa cells with resistance indices of 2.45, 2.26, 3.46, 1.88, and 1.85 respectively. In HEC-1-A cells, the resistance indices for doxorubicin, cisplatin, paclitaxel, raltitrexed, and oxaliplatin were found to be 1.46, 1.78, 2.33, 2.009, and l. 075 respectively (Table 3, 4). Furthermore, we calculated the IC_{50} of paclitaxel in HeLa and HEC-1-A was 7.457 nmol/L and 3.213 nmol/L, respectively (Figure 5c, d). Notably, after overexpression of BMI1, HeLa and HEC-1-A showed 3.4- and 2.33-fold resistance to paclitaxel, higher than that of other drugs (Table 3, 4). To investigate the potential role of BMI1 as a pivotal gene in paclitaxel tolerance, we examined the IC_{50} values of HeLa and HEC-1-A cell lines with varying levels of BMI1 expression upon exposure to paclitaxel. The results showed that the IC_{50} value was significantly higher in both HeLa and HEC-1-A cells overexpressing BMI1 compared to their respective controls. In addition, IC_{50} values gradually increased, corresponding to increased BMI1 expression levels. Moreover, transfection of siBMI1 resulted in further reduction of the IC_{50} value for both cell lines (Figure 5e, f). Consequently, targeting BMI1 may potentially serve as an effective strategy to delay the development of paclitaxel resistance.

Table 3 Sensitivity of HeLa cell line overexpressing BMI1 to antitumor drugs （n=3，$\bar{x}\pm s$）

Drugs	IC_{50}/(nmol·L^{-1})		Resistance multiple
	Negative control	BMI1 overexpression	
Doxorubicin	693.5±42.3	1 700±45.2	2.45
Cisplatin	849±95	1 920.3±185	2.26
Paclitaxel	7.45±0.868	25.04±1.576	3.40
Raltitrexed	63 840±6957	120 250±4737	1.88
Oxaliplatin	1 378.5±71	2 550±35	1.85

Table 4 Sensitivity of HEC−1−A cell line overexpressing BMI1 to antitumor drugs （n=3，$\bar{x}\pm s$）

Drugs	IC_{50}/(nmol·L^{-1})		Resistance multiple
	Negative control	BMI1 overexpression	
Doxorubicin	706.9±42	1 305.8±10	1.46
Cisplatin	1 564±41	2 784.5±36	1.78
Paclitaxel	3.2±0.161	7.472±0.167	2.33
Raltitrexed	125 800±4 666	252 800±2 828	2.009
Oxaliplatin	2 794±96	3 005±101	1.075

2.5 Additive effect of paclitaxel and BMI1 siRNA treatment on cancer cell apoptosis

As paclitaxel is a well-known antitumor drug that exerts its antitumor activity by modulating the apoptosis pathway of cells[18], we aim to investigate the regulatory effects of BMI1 on apoptosis through *in vitro* functional experiments. Firstly, flow cytometry was employed to assess the impact of BMI1 treatment on apoptosis levels in CC and EC. The results showed that the overexpression of BMI1 in CC and EC cells inhibited apoptosis, while the knockout of BMI1 increased apoptosis (Figure 6a). Additionally, Western blot analysis was conducted in HeLa and HEC-1-A cells treated with BMI1 siRNA or/and paclitaxel to explore whether BMI1 regulates apoptosis-related proteins. The findings revealed that compared to the control group, overexpression of BMI1 downregulated BAX expression, while knockdown of BMI1 upregulated BAX expression. Notably, there were no significant changes in BAX expression after paclitaxel treatment compared to DMSO treatment. Conversely, overexpression of BMI1 upregulated anti-apoptotic protein Bcl-2 expression which further decreased following paclitaxel treatment, indicating that paclitaxel promoted apoptosis by down-regulating Bcl-2 in HeLa and HEC-1-A cells. Moreover, both cell lines exhibited high expression levels of cleaved caspase3 (C-caspase3) and cleaved PARP1 (C-PARP1) after paclitaxel treatment, which are markers associated with apoptosis (Figure 6b, c). Subsequently, we investigated the main biological process of *BMI1* by performing Gene Ontology enrichments analyses which indicated its involvement primarily in mRNA

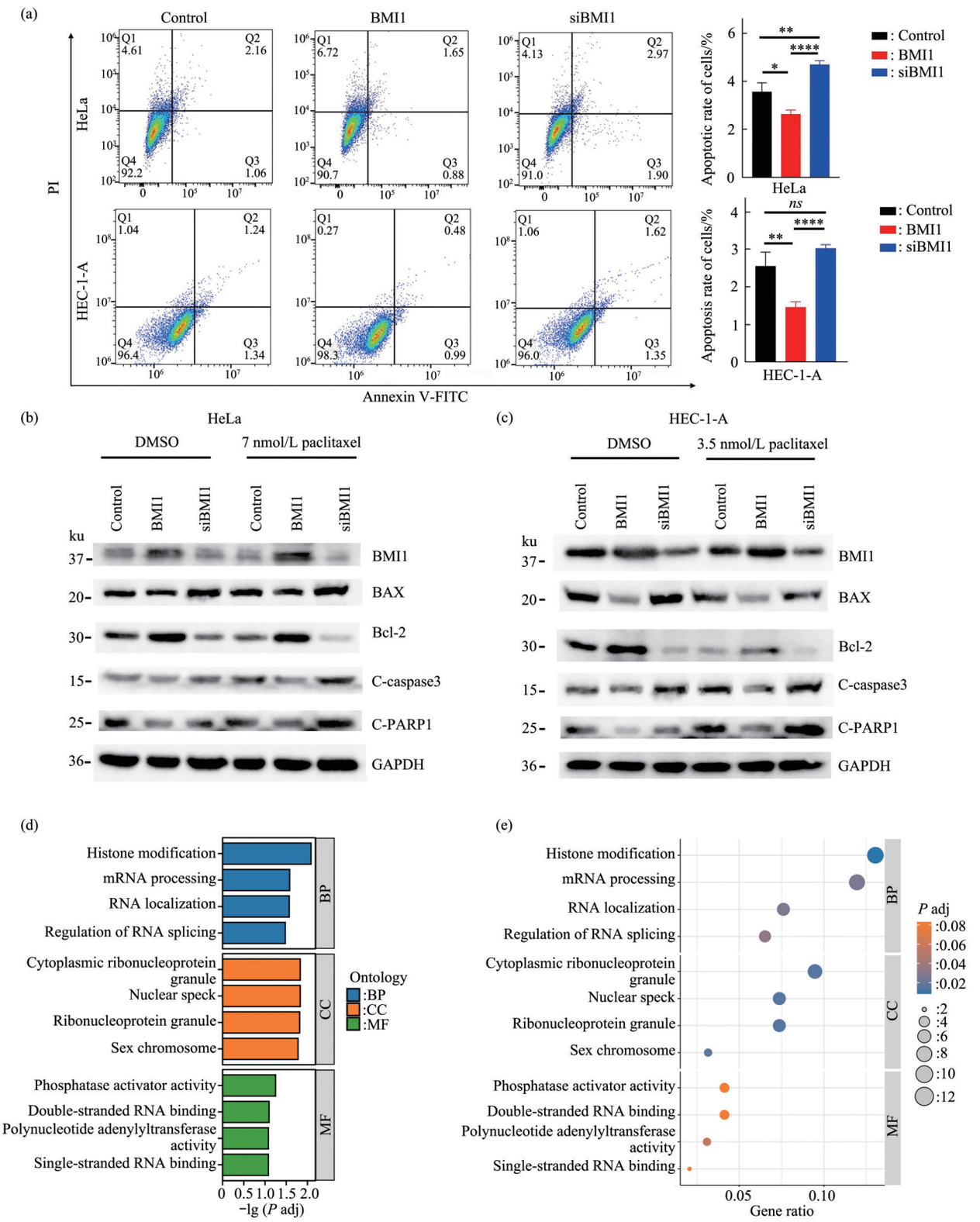

Fig. 6　Additive effect of paclitaxel and BMI1 siRNA treatment on cancer cell apoptosis

(a) Detection of apoptosis levels in HeLa and HEC-1-A cells flow cytometry. *ns* P>0.05; *P<0.05 **P<0.01; ****P<0.000 1. (b) HeLa cells were transfected with empty plasmid, BMI1 and siBMI1 plasmids, then DMSO or paclitaxel were added to the medium for 24 h treatment respectively, and the effects of BMI1 level on the expression of BAX, Bcl-2, C-caspase3 and C-PARP1 were detected by Western blot. (c) HEC-1-A cells were transfected with empty plasmid, BMI1 and siBMI1 plasmids, then DMSO or paclitaxel were added to the medium for 24 h treatment respectively, and the effects of BMI1 level on the expression of BAX, Bcl-2, C-caspase3 and C-PARP1 were detected by Western blot. (d, e) Gene Ontology enrichments, including biological process (BP), molecular function (MF), and cellular component (CC), were performed based on TCGA database by R package.

regulation (Figure 6d, e). Notably, Calao *et al*. [19] demonstrated that BMI1 could form a complex with other Polycomb complex proteins (Ring1A or Ring1B) and directly bind to p53 in neuroblastoma tumor cells, resulting in enhanced ubiquitination and degradation of p53. Moreover, the deficiency of BMI1 has been shown to elevate p53 levels, increase reactive oxygen species (ROS) concentrations abnormally, and enhance sensitivity to neurotoxic agents[20]. A previous study indicated that p53 could regulate the up-regulation of BAX expression and down-regulation of Bcl-2 expression to facilitate apoptosis[21-22]. Therefore, we speculate that *BMI1* may potentially interact with specific transcription factors to modulate apoptosis.

2.6 The synergic anti−growth effect of *BMI1* knockdown combined with paclitaxel treatment

In the above experiments, we established that BMI1 plays a pivotal role in paclitaxel resistance; consequently, knockdown of *BMI1* can reverse this resistance. To validate whether siBMI1 combined with paclitaxel could achieve the best inhibitory effect on HeLa and HEC-1-A cell proliferation and migration, we added paclitaxel to HeLa (7 nmol/L) and HEC-1-A (3.5 nmol/L) cells with *BMI1* knockdown or not. The results of the CCK-8 assay showed that cell growth and proliferation were dramatically decreased in HeLa and HEC-1-A cells with BMI1 knockdown compared to the respective controls. Significantly, the growth and proliferation of siBMI1-transfected HeLa and HEC-1-A cells treated with paclitaxel further decreased (Figure 7a, b). Similarly, in the colony formation assay, the number of average colony counts of the siBMI1 knockdown group of HeLa and HEC-1-A cells was sharply lower than the respective control, and the co-treatment of siBMI1 and paclitaxel had a more significant decrease in cell colony formation (Figure 7c, d). Consistently, the cell migration was similar (Figure 7e). These results suggest that *BMI1* knockdown may help CC and EC cells become sensitive to paclitaxel.

3 Discussion

High BMI1 expression is significantly associated with poor tumor differentiation, high clinical grade, lymph node metastasis, and poor prognosis of CC and EC and is an independent prognostic factor in CC[16]. In line with this evidence, our results also show that the protein level of BMI1 is overexpressed in CC and EC and supports the oncogenic role of BMI1 in the proliferation and migration of CC and EC cells. Moreover, overexpression of BMI1 can also lead to multidrug resistance in CC and EC cells. Co-administration of paclitaxel and BMI1 inhibition could significantly promote the apoptosis of CC and EC cells and significantly attenuate their cell viability.

Importantly, the pathological evidence that leads to the overexpression of BMI1 in EC and CC remains unknown. On the one hand, there is advancing evidence indicating that BMI1 could be regulated by some miRNAs, a group of endogenous noncoding single-stranded RNAs that negatively regulate the expression of BMI1 genes in several malignant tumors but without CC and EC. We further detected these miRNAs using the GEO database. Indeed, miR-203 was significantly downregulated in CC (Table S3). This may lead to high BMI1 expression in CC. The relationship between miR-203 and BMI1 in CC warrants further investigation other miRNAs, such as miR-200 and miR-218, in CC and EC were not similar to previous findings in other cancers (Table S3) [23-26]. However, there are limited reports indicating post-translational modification (PTM)-mediated regulation of BMI1, such as ubiquitination, which requires urgent exploration in the future.

Most patients with CC and EC are effectively treated with surgery in the early stages. However, patients with advanced or recurrent disease show a high rate of chemoresistance. Strategies for the development of more effective and efficient therapies are urgently required in this field. The link between BMI1 and chemoresistance has been elaborated in several cancers, including head and neck squamous cell carcinoma (HNSCC). The idea that cancer stem-like cells (CSCs) drive cancer metastasis and chemoresistance is well established. For instance, the direct inhibition of BMI1 abrogates the self-renewal process of head and neck cancer stem cells and increases tumor sensitivity to cisplatin[27]. We and others have shown that *BMI1* knockdown can increase the drug efficiency without an explicit explanation. Only one report has shown that inhibition of BMI1 reduces the migration and invasion of EC cells *in vivo* and *in vitro* by upregulating the expression levels of E-cadherin and downregulating N-cadherin, vimentin, and SLUG. Therefore, the underlying mechanism of

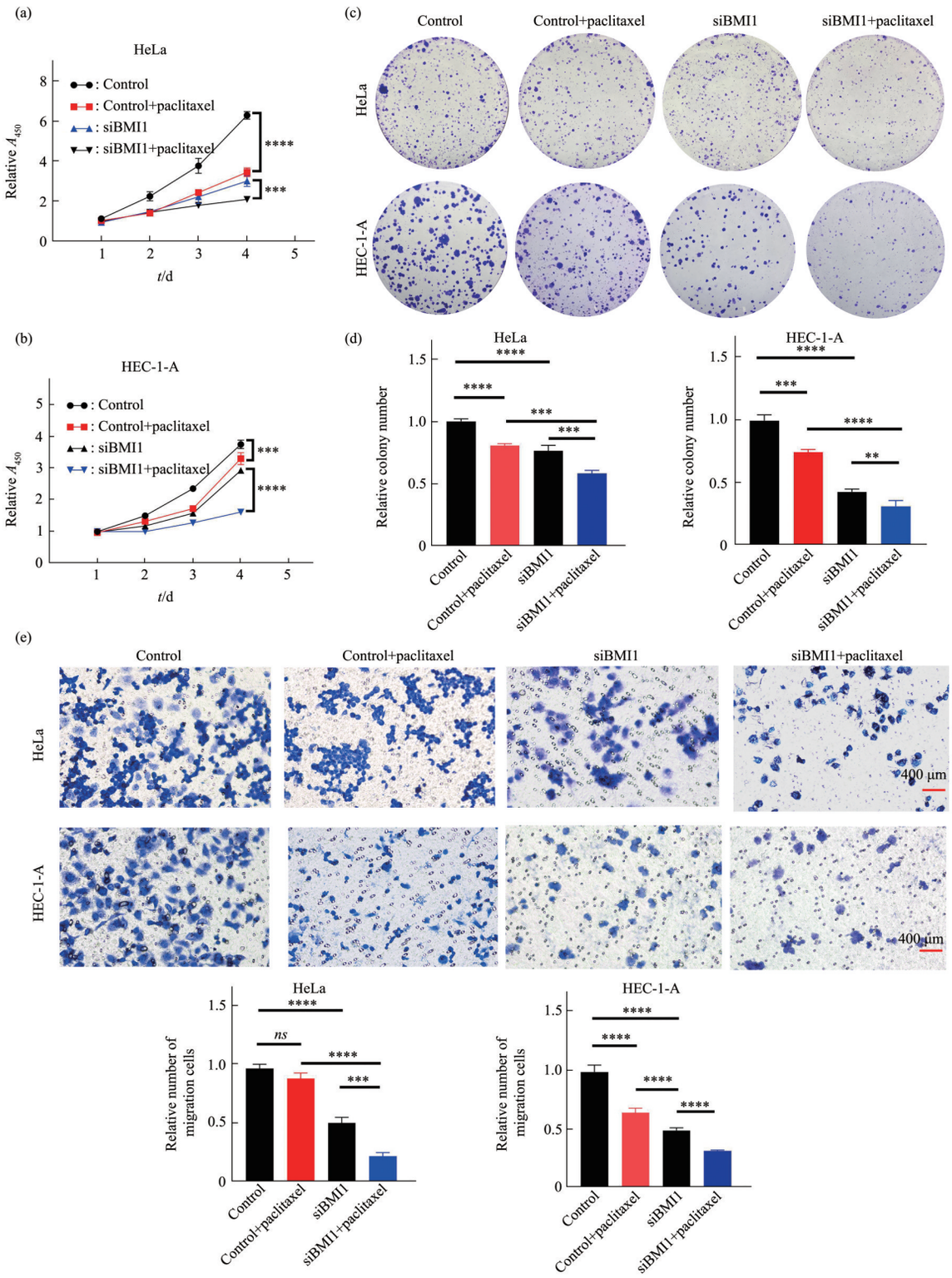

Fig. 7　BMI1 expression promotes paclitaxel resistance in HeLa and HEC−1−A cells

(a) Cell proliferation assay of HeLa cells transfected with empty plasmids and siBMI1 plasmids. 7 nmol/L paclitaxel was added after transfected 24 h and remained for 6 hours. Statistical analysis was performed using two-way ANOVA. ***P<0.001; ****P<0.000 1. (b) Cell proliferation assay of HEC-1-A cells transfected with empty plasmids and siBMI1 plasmids. 3.5 nmol/L paclitaxel was added after transfected 24 h and remained for 6 h. Statistical analysis was performed using two-way ANOVA. ***P<0.001; ****P<0.000 1. (c) Cell colony formation assay of HeLa and HEC-1-A cells transfected with empty plasmids and siBMI1 plasmids and remained for 6 h. (d) Statistical results of cell colony formation assay of HeLa and HEC-1-A cells, all data shown are *mean*±*SD* (n=3). **P<0.01; ***P<0.001; ****P<0.000 1. (e) Transwell migration assay of HeLa and HEC-1-A cells transfected with empty plasmids and siBMI1 plasmids. Paclitaxel was added after transfected 24 h. Statistical analysis was performed using one-way ANOVA. *ns*: P>0.05; ***P <0.001; ****P<0.000 1.

BMI1-associated drug resistance requires further exploration in CC and EC.

The BMI1 inhibitor, from first-generation PTC-209 to second-generation PTC-028, shows potential effects on the inhibition of cancer cell viability[11-12]. Although the roles of several key inhibitors have been comprehensively summarized in different tumor cell models, only one inhibitor has been tested in CC and EC respectively[28]. Notably, PTC-596 is the only one BMI1 inhibitor now in the clinical phase 1 trial of diffuse intrinsic pontine glioma and leiomyosarcoma[29-30], but there is a lack of a unique drug to be used in clinical practice to target BMI1 specifically. Moreover, from the laboratory bench to the clinical bed, the effective function and toxic side effects should also be considered in a carcinosarcoma xenograft model.

4 Conclusion

This study confirmed that BMI1 protein is overexpressed in cancer tissues of CC and EC compared with normal tissues, promoting the proliferation and migration of CC and EC cells. BMI1 also has been demonstrated increased the resistance of CC and EC cells to a variety of anticancer drugs, including paclitaxel. Additionally, there was a positive correlation observed between BMI1 and the anti-apoptotic factor Bcl-2. Silencing *BMI1* resulted in increased sensitivity of CC and EC cells to paclitaxel by augmenting pro-apoptotic regulation.

Acknowledgements We thank Ms. DAI Zhen-Zhen（958025950@qq.com） and Mr. FANG Lai-Fu（12576890@qq.com） from the Affiliated People's Hospital of Ningbo University for their technical assistance in the analysis of IHC scores.

Data availability The datasets analysed during the current study are available in the UCSC platform（https://xenabrowser.net/） and UALCAN platform（http://ualcan.path.uab.edu/index.html） repository.

Supplementary Available online (http://www.pibb.ac.cn or http://www.cnki.net):
PIBB_20230207_Figure_S1.pdf
PIBB_20230207_Figure_S2.pdf
PIBB_20230207_Table_S1.pdf
PIBB_20230207_Table_S2.pdf
PIBB_20230207_Table_S3.pdf

References

[1] Liu Y, Fan P, Yang Y, *et al*. Human papillomavirus and human telomerase rna component gene in cervical cancer progression. Sci Rep, 2019, **9**(1): 15926

[2] Bray F, Ferlay J, Soerjomataram I, *et al*. Global cancer statistics 2018: globocan estimates of incidence and mortality worldwide for 36 cancers in 185 countries. CA Cancer J Clin, 2018, **68**(6): 394-424

[3] Siegel R L, Miller K D, Jemal A. Cancer statistics, 2019. CA Cancer J Clin, 2019, **69**(1): 7-34

[4] Falcetta F S, Medeiros L R, Edelweiss M I, *et al*. Adjuvant platinum-based chemotherapy for early stage cervical cancer. Cochrane Database Syst Rev, 2016, **11**(11): Cd005342

[5] Datta N R, Stutz E, Gomez S, *et al*. Efficacy and safety evaluation of the various therapeutic options in locally advanced cervix cancer: a systematic review and network meta-analysis of randomized clinical trials. Int J Radiat Oncol Biol Phys, 2019, **103**(2): 411-437

[6] Alqahtani F Y, Aleanizy F S, El Tahir E, *et al*. Paclitaxel. Profiles Drug Subst Excip Relat Methodol, 2019, **44**: 205-238

[7] Glinsky G V, Berezovska O, Glinskii A B. Microarray analysis identifies a death-from-cancer signature predicting therapy failure in patients with multiple types of cancer. J Clin Invest, 2005, **115**(6): 1503-1521

[8] Häyry V, Tynninen O, Haapasalo H K, *et al*. Stem cell protein bmi-1 is an independent marker for poor prognosis in oligodendroglial tumours. Neuropathol Appl Neurobiol, 2008, **34**(5): 555-563

[9] Bhattacharya R, Nicoloso M, Arvizo R, *et al*. Mir-15a and mir-16 control bmi-1 expression in ovarian cancer. Cancer Res, 2009, **69**(23): 9090-9095

[10] Hoenerhoff M J, Chu I, Barkan D, *et al*. Bmi1 cooperates with h-ras to induce an aggressive breast cancer phenotype with brain metastases. Oncogene, 2009, **28**(34): 3022-3032

[11] Kreso A, Van Galen P, Pedley N M, *et al*. Self-renewal as a therapeutic target in human colorectal cancer. Nat Med, 2014, **20**(1): 29-36

[12] Buechel M, Dey A, Dwivedi S K D, *et al*. Inhibition of bmi1, a therapeutic approach in endometrial cancer. Mol Cancer Ther, 2018, **17**(10): 2136-2143

[13] Xu R, Chen L, Yang W T. Aberrantly elevated bmi1 promotes cervical cancer tumorigenicity and tumor sphere formation *via* enhanced transcriptional regulation of *sox2* genes. Oncol Rep, 2019, **42**(2): 688-696

[14] Li J, Vangundy Z, Poi M. Ptc209, a specific inhibitor of bmi1, promotes cell cycle arrest and apoptosis in cervical cancer cell lines. Anticancer Res, 2020, **40**(1): 133-141

[15] Zaczek A, Jóźwiak P, Ciesielski P, *et al*. Relationship between polycomb-group protein bmi-1 and phosphatases regulating akt phosphorylation level in endometrial cancer. J Cell Mol Med,

2020, **24**(2): 1300-1310

[16] Sun X, Xu H, Dai T, *et al*. Alantolactone inhibits cervical cancer progression by downregulating bmi1. Sci Rep, 2021, **11**(1): 9251

[17] Jin X, Wang J, Li Q, *et al*. Spop targets oncogenic protein zbtb3 for destruction to suppress endometrial cancer. AmJ Cancer Res, 2019, **9**(12): 2797-2812

[18] Wang T H, Wang H S, Soong Y K. Paclitaxel-induced cell death: Where the cell cycle and apoptosis come together. Cancer, 2000, **88**(11): 2619-2628

[19] Calao M, Sekyere E O, Cui H J, *et al*. Direct effects of bmi1 on p53 protein stability inactivates oncoprotein stress responses in embryonal cancer precursor cells at tumor initiation. Oncogene, 2013, **32**(31): 3616-3626

[20] Chatoo W, Abdouh M, David J, *et al*. The polycomb group gene bmi1 regulates antioxidant defenses in neurons by repressing p53 pro-oxidant activity. J Neurosci, 2009, **29**(2): 529-542

[21] Wei H, Wang H, Wang G, *et al*. Structures of p53/bcl-2 complex suggest a mechanism for p53 to antagonize bcl-2 activity. Nat Commun, 2023, **14**(1): 4300

[22] Shen Y, White E. P53-dependent apoptosis pathways. Adv Cancer Res, 2001, **82**: 55-84

[23] Wu J, Jiang Z M, Xie Y, *et al*. Mir-218 suppresses the growth of hepatocellular carcinoma by inhibiting the expression of proto-oncogene bmi-1. J BUON, 2018, **23**(3): 604-610

[24] Fu W M, Tang L P, Zhu X, *et al*. Mir-218-targeting-bmi-1 mediates the suppressive effect of 1,6,7-trihydroxyxanthone on liver cancer cells. Apoptosis, 2015, **20**(1): 75-82

[25] Xu L, Lin J, Deng W, *et al*. Ezh2 facilitates bmi1-dependent hepatocarcinogenesis through epigenetically silencing microrna-200c. Oncogenesis, 2020, **9**(11): 101

[26] Xu Z, Zhou Z, Zhang J, *et al*. Targeting bmi-1-mediated epithelial-mesenchymal transition to inhibit colorectal cancer liver metastasis. Acta Pharm Sin B, 2021, **11**(5): 1274-1285

[27] Herzog A E, Warner K A, Zhang Z, *et al*. The il-6r and bmi-1 axis controls self-renewal and chemoresistance of head and neck cancer stem cells. Cell Death Dis, 2021, **12**(11): 988

[28] Xu J, Li L, Shi P, *et al*. The crucial roles of bmi-1 in cancer: implications in pathogenesis, metastasis, drug resistance, and targeted therapies. Int J Mol Sci, 2022, **23**(15): 8231

[29] Jernigan F, Branstrom A, Baird J D, *et al*. Preclinical and early clinical development of ptc596, a novel small-molecule tubulin-binding agent. Mol Cancer Ther, 2021, **20**(10): 1846-1857

[30] Shapiro G I, O'mara E, Laskin O L, *et al*. Pharmacokinetics and safety of ptc596, a novel tubulin-binding agent, in subjects with advanced solid tumors. Clin Pharm Drug Dev, 2021, **10**(8): 940-949

*BMI1*基因下调使宫颈癌和子宫内膜癌对紫杉醇敏感*

赵奕婷[1,2,3)**]　林　燕[3)**]　杨玮丽[2,3)**,***]　陈　俊[1,3)***]

([1)] 宁波大学附属人民医院肿瘤放化疗科，宁波 315000；

[2)] 宁波大学附属人民医院妇科，宁波 315000；

[3)] 宁波大学医学部生物化学与分子生物学系，浙江省病理生理学重点实验室，宁波 315000）

摘要　目的　研究B细胞特异性莫洛尼鼠白血病病毒插入位点1（*BMI1*）基因对宫颈癌及子宫内膜癌增殖浸润及紫杉醇耐受的影响及其机制。**方法**　首先利用Cbioportal、TCGA和CPTAC数据库分析*BMI1*基因在宫颈癌和子宫内膜癌中的突变及表达情况。接着对人宫颈癌组织样本和人子宫内膜癌组织样本中BMI1的蛋白质表达水平进行免疫组化分析。采用蛋白质印迹法（Western blot）检测BMI1敲低后宫颈癌及子宫内膜癌细胞中BMI1下游调控因子的蛋白质水平变化。此外，通过细胞功能实验研究了BMI1在宫颈癌HeLa及子宫内膜癌HEC-1-A细胞中的功能。最后，通过实验评估si*BMI1*联合紫杉醇治疗的协同抗生长作用。**结果**　数据库分析结果显示，BMI1在1.5%的子宫颈癌患者及1.9%的子宫内膜癌的患者中存在不同程度的扩增、错义及剪接突变。此外，高mRNA水平的BMI1与宫颈癌的病理类型相关，且高蛋白质水平的BMI1与子宫内膜癌的病理类型和肿瘤分级及较低的生存率相关。进一步的免疫组化分析发现，与正常组织相比，宫颈癌和子宫内膜癌组织中BMI1蛋白水平表达升高，且与肿瘤的病理分化及浸润深度相关。药物敏感性实验显示，BMI1过表达导致HeLa及HEC-1-A细胞对多种抗癌药物的敏感性下降，其中包括紫杉醇。为了进一步分析BMI1与紫杉醇耐受的关系，通过Western blot检测*BMI1*敲除后HeLa及HEC-1-A细胞中BMI1下游因子的蛋白质水平变化。结果显示，抗凋亡相关蛋白Bcl-2随着*BMI1*的敲低而表达水平下降，而促凋亡相关蛋白BAX则显著升高。此外，细胞功能实验结果显示，体外过表达BMI1可促进HeLa及HEC-1-A细胞的增殖和迁移，且BMI1低表达的HeLa及HEC-1-A细胞对紫杉醇更敏感。**结论**　BMI1在宫颈癌和子宫内膜癌患者的肿瘤组织中过表达，BMI1的下调通过调控凋亡通路使CC和EC细胞对紫杉醇更加敏感。

关键词　宫颈癌，子宫内膜癌，BMI1，Bcl-2，紫杉醇

中图分类号　R737.33　　**DOI**：10.16476/j.pibb.2023.0207

* 浙江省医药卫生科技计划（2019RC274），浙江省病理生理重点实验室开放基金（202306），宁波市自然科学基金（2021J017），宁波市公益性科技计划（2021S116）和浙江省中医药科技计划（2021ZB265）资助项目。

** 并列第一作者。

*** 通讯联系人。

杨玮丽　Tel：0574-87017139，E-mail：gjywl-0506@163.com

陈俊　Tel：0574-87017551，E-mail：cjcj992@163.com

收稿日期：2023-05-24，接受日期：2023-10-16